

Decay spectroscopy of $^{179}_{82}\text{Pb}_{97}$ and evidence for a $9/2^-$ intruder state in $^{179}_{81}\text{Tl}_{98}$

H. Badran,^{1,*} C. Scholey,¹ J. Uusitalo,¹ K. Auranen,^{1,†} T. Grahn,¹ P. T. Greenlees,¹ A. Herzán,^{1,‡} U. Jakobsson,^{2,§} R. Julin,¹ S. Juutinen,¹ J. Konki,¹ M. Leino,¹ M. J. Mallaburn,^{1,3} J. Pakarinen,¹ P. Papadakis,¹ J. Partanen,¹ P. Peura,^{1,||} P. Rakkila,¹ M. Sandzelius,¹ J. Sarén,¹ J. Sorri,^{1,¶} and S. Stolze¹

¹University of Jyväskylä, Department of Physics, PO Box 35, FI-40014, Jyväskylä, Finland

²Department of Physics, KTH-Royal Institute of Technology, SE-10691 Stockholm, Sweden

³University of Manchester, Manchester M13 9PL, United Kingdom

(Received 31 July 2017; revised manuscript received 13 November 2017; published 18 December 2017)

The very neutron-deficient isobars ^{179}Pb and ^{179}Tl have been produced using the fusion-evaporation reactions $^{104}\text{Pd}(^{78}\text{Kr}, x\text{pyn})$, where $x \leq 1$ and $y \geq 2$. The gas-filled separator RITU was employed to transport and separate the recoiling nuclei of interest from the scattered beam and unwanted products. The GREAT spectrometer was used to study the decay properties through α - α and α - γ correlations, which has allowed the ground state of ^{179}Pb to be assigned as $I^\pi = 9/2^-$. The decay of ^{179}Pb was measured to have an α -particle energy and half-life of $E_\alpha = 7348(5)$ keV and $t_{1/2} = 2.7(2)$ ms, respectively. A search for a $\nu i_{13/2}$ state in ^{179}Pb was performed, but only a limit of excitation energy and half-life was obtained. In ^{179}Tl a $t_{1/2} = 114^{+18}_{-10}$ ns isomeric state, likely at an excitation energy of 904.5(9) keV, was identified and is tentatively assigned to be a $9/2^-$ proton intruder state.

DOI: 10.1103/PhysRevC.96.064314

I. INTRODUCTION

The α -decay fine structure and hindrance factors of very neutron-deficient nuclei are powerful tools for determining spins and parities of low-lying states. Identifying single-particle states around Pb reveals the states responsible for driving the nuclear shape from sphericity at low excitation energies, even though Pb at $Z = 82$ is a closed shell. Such information is certainly most important in this region of shape coexistence [1,2].

The neutron-deficient region of the nuclear chart, from Pb at $Z = 82$, down to $N = 82$ uniquely allows the study of α -decay chains between two closed shells. α -decay chains themselves allow the study of nuclear structure effects when the proton and neutron numbers are changing, but the number of valence nucleons remains constant. In the α -decay chain of ^{179}Pb the $\nu f_{7/2}$ and $\nu h_{9/2}$ orbitals are found near the Fermi surface, along with the $\nu i_{13/2}$ unique-parity shell-model intruder orbital, which in most cases is an isomeric state decaying via an $M2$ transition to the $\nu h_{9/2}$ state. The behavior of the $9/2^-$ and $13/2^+$ states, the excitation energy and the reduced-transition probability of the ^{179}Pb α -decay chain partners, ^{171}Pt , ^{167}Os , and ^{163}W have been reported by Scholey *et al.* [3], revealing a striking consistency between the level energy differences and $B(M2)$ values.

The α decay of ^{179}Pb has been observed previously by Andreyev *et al.* [4] and contrary to the lighter members of the

α -decay chain, was tentatively assigned as $I^\pi = 9/2^-$ ground state. A total of 12 events over a broad energy range were seen and hence it was concluded that the observed α decay must feed the excited $9/2^-$ state in ^{175}Hg [5] due to the broad energy distribution of decay events, but no α - γ correlations were observed. The present paper confirms the initial finding with more accurate energy and half-life values of the ^{179}Pb α decay. Also, the assignment of the ground-state spin and parity as $I^\pi = 9/2^-$ is confirmed through the observation of an 80 keV γ -ray transition following the $\Delta l = 0$ α decay of ^{179}Pb to the first excited $I^\pi = 9/2^-$ state in ^{175}Hg [5]. No evidence for the $\nu i_{13/2}$ state in ^{179}Pb was observed.

In studying the neighboring isobar to ^{179}Pb , ^{179}Tl the protons near the Fermi surface are revealed. The neutron-deficient Tl ($Z = 81$) isotopes play a vital role in understanding the shape coexistence phenomena. The intruder $9/2^-$ and $13/2^+$ excited states originating from one-particle one-hole (1p-1h) excitations to the $\pi h_{9/2}$ and $\pi i_{13/2}$ orbitals, respectively, are both observed at low energies in the odd-mass $^{183-195}\text{Tl}$ isotopes [6–9]. In fact, the $9/2^-$ state, which is assigned to have an oblate-deformed shape is known to be present along the isotopic chain down to ^{181}Tl [10].

The ^{179}Tl ($N = 98$) isotope is located 24 neutrons away from the stable isotope ^{203}Tl . It has a ground state configuration of $\pi(s_{1/2})^{-1}$, which has recently been confirmed by a laser-spectroscopy study [11]. In addition, it is known to have an $\pi(h_{11/2})^{-1}$ isomeric state with a half-life of $t_{1/2} = 1.46(4)$ ms, that α decays to a $\pi(h_{11/2})^{-1}$ isomeric state in ^{175}Au [4]. The present work reports on a tentative observation of the ($9/2^-$) proton intruder state for the first time in ^{179}Tl and extends the level-energy systematics of odd- A Tl isotopes further beyond the proton drip-line.

II. EXPERIMENTAL DETAILS

The neutron-deficient isotopes of interest were produced using the fusion-evaporation reactions $^{104}\text{Pd}(^{78}\text{Kr}, 3n)^{179}\text{Pb}$

*hussam.h.badran@jyu.fi

[†]Present address: Argonne National Laboratory, 9700 Cass Ave, Lemont, IL 60439, United States.

[‡]Present address: Oliver Lodge Laboratory, University of Liverpool, Liverpool L69 7ZE, United Kingdom.

[§]Present address: Laboratory of Radiochemistry, Department of Chemistry, P.O. Box 55, FI-00014 University of Helsinki, Finland.

^{||}Present address: Helsinki Institute of Physics, University of Helsinki, P.O. Box 64, 00014 Helsinki, Finland.

[¶]Present address: Finnish Defence Forces, Logistics Command.

and $^{104}\text{Pd}(^{78}\text{Kr}, p2n)^{179}\text{Tl}$, at the Accelerator Laboratory of the University of Jyväskylä, Finland. A heavy-ion beam of $^{78}\text{Kr}^{15+}$ with an energy of 358 MeV was impinged on a self-supporting rotating ^{104}Pd target with a thickness and enrichment of $745\ \mu\text{g}/\text{cm}^2$ and 95.25%, respectively. A $34\ \mu\text{g}/\text{cm}^2$ thick carbon charge-reset foil was positioned behind the target. The beam intensity during the 224 h of irradiation was, on average 140 pA. The evaporation residues of interest (recoils) formed in the fusion-evaporation reactions were separated from the beam and unwanted reaction products using the gas-filled separator RITU [12] and transported to its focal plane, where the GREAT spectrometer [13] is located.

In the GREAT spectrometer recoils passed through a multiwire proportional counter (MWPC) and implanted into a set of two adjacent, $300\ \mu\text{m}$ thick double-sided silicon strip detectors (DSSD). Both DSSDs have an active area of $60 \times 40\ \text{mm}^2$ and a strip pitch of 1 mm on both faces yielding 4800 pixels. The DSSD strips were calibrated internally using the known α -particle energies of $^{176,179}\text{Hg}$ and ^{176}Pt , from Refs. [14–16], respectively (see Fig. 1). A $700\ \mu\text{g}/\text{cm}^2$ degrader of aluminized mylar was positioned between the DSSDs and MWPC to reduce low-energy reaction products in the implantation detectors.

A 15 mm thick planar double-sided germanium strip detector with a $120 \times 60\ \text{mm}^2$ active area and strip pitch of 5 mm was positioned directly behind the DSSDs inside the vacuum chamber. The low-energy γ rays and x rays were observed using the planar detector. In addition, in the present experiment it was used to veto energetic light-particles that pass through the DSSDs, depositing an amount of energy that overlaps with the α -particle energies from the nuclei of interest. One large volume and two EUROGAM type clover [17] germanium detectors surround the vacuum chamber of the GREAT spectrometer. The clover detectors were set in order to measure high-energy γ rays and x rays.

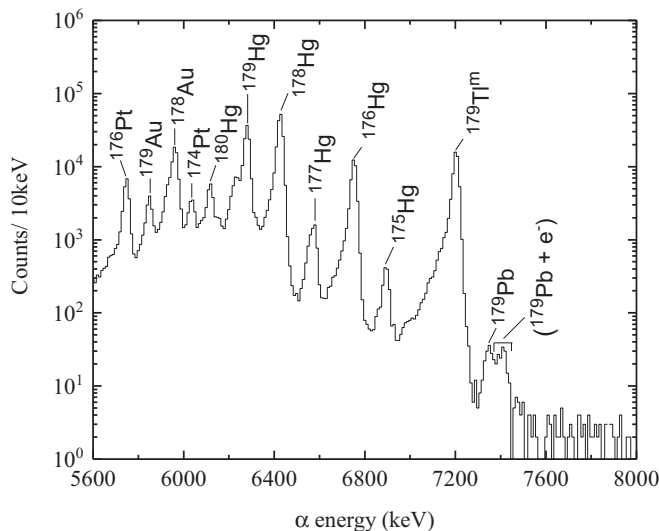


FIG. 1. Energy spectrum of α -particles correlated within a maximum search time of 20 ms following a recoil implant within the same pixel in the DSSDs at the focal plane of RITU, vetoed by the gas counter (MWPC) and the planar Ge detector.

The data from each detector channel were recorded independently using the triggerless total data readout (TDR) [18] data acquisition system. All the events were time-stamped with a precision of 10 ns by using a 100 MHz clock. The data analysis was performed using the GRAIN software package [19].

A more detailed description of the experimental setup is presented in Ref. [20].

III. EXPERIMENTAL RESULTS

A. Decay spectroscopy of ^{179}Pb

Figure 1 shows the energy spectrum of all recoil-correlated decay events detected in the DSSDs within a 20 ms correlation time and vetoed by the MWPC and the planar Ge detector. The spectrum is dominated by proton and α -particle evaporated products, due to the proximity of the proton drip line.

A two-dimensional plot of α -particle energy parent-child correlations is illustrated in Fig. 2(a). Maximum correlation search times of 20 ms and 45 ms were used for the recoil-parent and parent-child correlation events, respectively.

The group of α -decay activity between 7320–7450 keV in Figs. 1 and 2 corresponds to the α decay of ^{179}Pb produced via the $3n$ -exit channel. The technique of recoil- α_1 (parent)- α_2 (child)- α_3 (grandchild) correlations was applied to confirm the initial findings by Andreyev *et al.* [4]. The α decay of ^{179}Pb was identified using the known energy and half-life of the child ^{175}Hg and grandchild ^{171}Pt α decay [21]. In total 105 ^{179}Pb α -decay events correlated with its child ^{175}Hg , [$E_{\alpha_2} = 6898(4)$ keV and $t_{1/2} = 9.6(4)$ ms], were observed. The α -particle energy for ^{175}Hg reported here from the present work is consistent within errors with values reported in Refs. [22,23]. Parent-child α -decay correlations of $^{179}\text{Tl}^m$ [4], ^{176}Hg [14], ^{175}Hg [21], and ^{178}Pb [20] can also be seen in Fig. 2(a).

The production cross section of ^{179}Pb is estimated to be $\sigma \approx 200$ pb taking into account the calculated RITU transmission efficiency [24], DSSD coverage, and α -particle full-energy detection efficiency of 50%, 70%, and 55%, respectively.

Figure 2(b) shows a two-dimensional energy plot of parent- α decay versus γ -ray energies, with the MWPC and planar Ge detector veto applied to the α -decay events. A 20 ms correlation time was applied for an α_1 decay after a recoil implant, while the γ -ray energies are those detected in both the clovers and planar Ge detectors within a 750 ns time window subsequent to an α_1 decay, with the aforementioned time condition. In total, 13 γ -ray events of $E_\gamma = 80.0(5)$ keV were detected in prompt coincidence with an α_1 decay having an energy of 7348(5) keV, which is assigned to ^{179}Pb as shown in Fig. 2(c). An 80 keV transition was observed previously in ^{175}Hg by O'Donnell *et al.* [5]. This transition de-excites the first excited state in ^{175}Hg , which has a spin and parity of $I^\pi = 9/2^-$ and feeds the $7/2^-$ ground state, hence the transition has an $M1$ character. In addition, the $9/2^-$ excited state is populated by the decay of a $0.34(3)\ \mu\text{s}$ $13/2^+$ isomeric state via an $M2$ transition also reported in Ref. [5] (see Fig. 6). The strong coincidence between the α decay of ^{179}Pb and the 80 keV γ ray transition in ^{175}Hg observed in

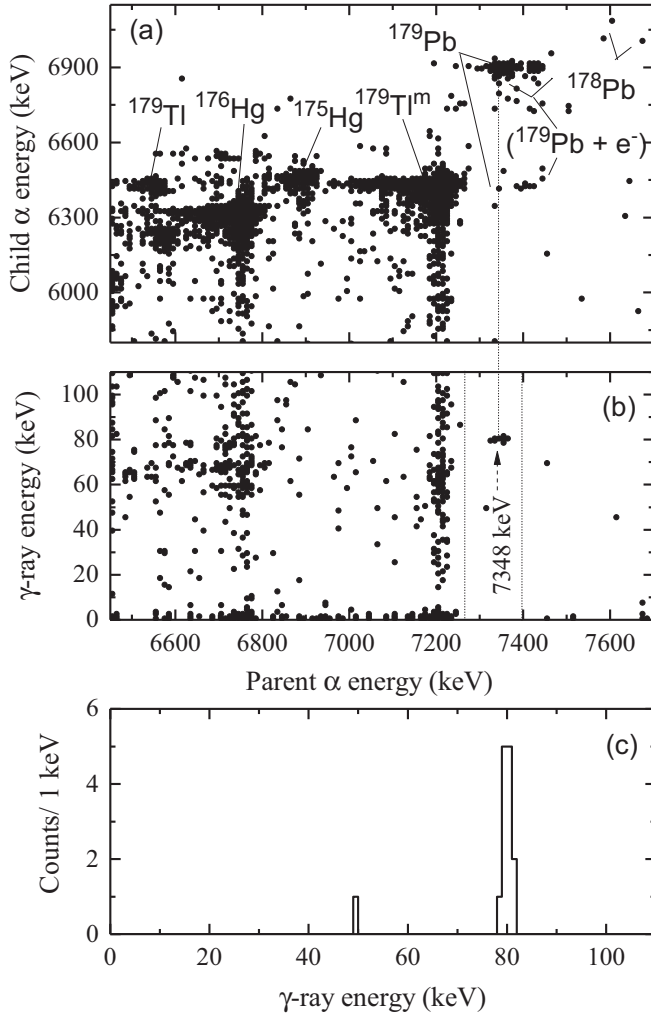


FIG. 2. (a) A matrix of parent and child α -particle energies vetoed by the MWPC and planar. Maximum searching times of 20 ms and 45 ms were used for the recoil-parent pairs and the parent-child pairs, respectively; (b) α - γ energy matrix vetoed by MWPC and planar Ge detector within a 20 ms correlation time for recoil-parent pairs; (c) a γ -ray energy spectrum following the 7348(5) keV α decay of ^{179}Pb within a 750 ns time window. The dashed line from (a) to (b) represents the α decay of ^{179}Pb 's ground state. The dashed lines in (b) represent the energy limits to produce spectrum (c).

the present work in addition to the hindrance factor value (discussed later in Sec. IV A), firmly assigns the ground-state spin and parity of ^{179}Pb to be $I^\pi = 9/2^-$. The α -particle energy was deduced from the coincidence discussed above, to be $E_\alpha = 7348(5)$ keV for the $9/2^-$ ground state decay of ^{179}Pb .

The theoretical total internal-conversion coefficient for an 80 keV $M1$ transition in ^{175}Hg is $\alpha_{\text{tot}} = \lambda_e/\lambda_\gamma = 2.74(2)$ [25], which is mainly due to L and M electron conversion as the K -binding energy $B_k = 88.1$ keV [26] for mercury is larger than 80 keV. In fact, L electrons dominate by $L/M = 4.29(9)$ [25] and have an energy of $E_e^L \simeq 65.17$ keV and $E_e^M \simeq 76.44$ keV for the L and weaker M internal-conversion electrons lines [26], respectively.

The energy sum of the ^{179}Pb α -particle and conversion electrons ($E_\alpha + E_e$) in the same pixel of the DSSDs was observed as shown in Figs. 1 and 2(a). Either a full energy of $E_\alpha(7348) + E_e^L(65.17) \simeq 7413(5)$ keV or $E_\alpha(7348) + E_e^M(76.44) \simeq 7424(5)$ keV or part of it (escape events) will deposit in the DSSDs. In addition, the group of events around ~ 7356 keV and ~ 7440 keV, can be explained as being due to the additional summing with Hg x rays (< 15 keV) and Auger electrons. The intensity ratio of ^{179}Pb α -particle and the summing of electron energies in Figs. 2(a), 1, and 3 (inset) is in agreement with the theoretical α_{tot} value [25].

Figure 3 reveals the logarithmic-time difference spectrum between the implanted recoils in the DSSDs and the α decay of ^{179}Pb . Maximum correlation searching times of 20 ms and 45 ms for recoil- $\alpha_1(^{179}\text{Pb})$ and $\alpha_1(^{179}\text{Pb})$ - $\alpha_2(^{175}\text{Hg})$, respectively, were used to produce the plot in Fig. 3. The maximum value of the curve (shown in red color online), yields $\ln(1/\lambda)$ [27], where λ is the decay time constant. The half-life of ^{179}Pb could thus be extracted as $t_{1/2} = 2.7(2)$ ms.

A [recoil- γ]- $\alpha_1(^{179}\text{Pb})$ and [recoil- e^-]- $\alpha_1(^{179}\text{Pb})$ analysis were performed in order to search for the $13/2^+$ isomeric state in ^{179}Pb . No evidence for the $13/2^+$ state either depopulating the ground state of ^{179}Pb or α decaying to $13/2^+$ state in ^{175}Hg was found.

B. Proton ($9/2^-$) intruder state in ^{179}Tl

In order to search for γ rays depopulating isomeric states in ^{179}Tl a technique of [recoil- γ]- α_1 - α_2 correlations was applied, where α_1 and α_2 in this case are the parent ^{179}Tl and child ^{175}Au α decays after a recoil implant within the same pixel in the DSSDs, respectively.

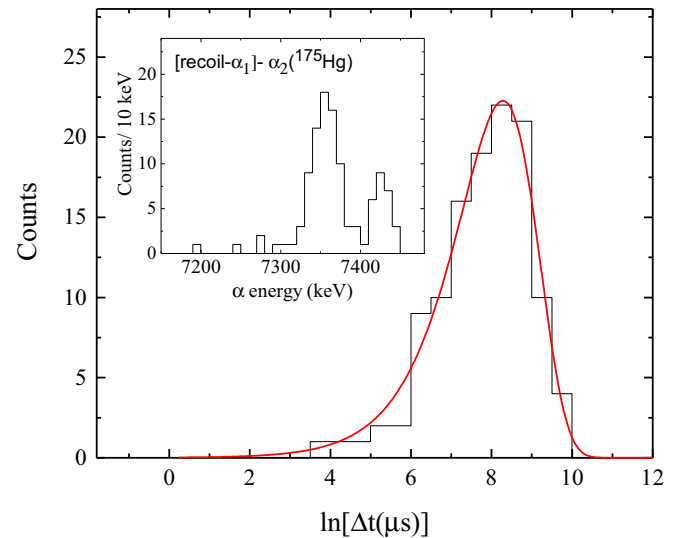


FIG. 3. Time spectrum of the ^{179}Pb α decay, which shows the logarithm of the time difference (Δt) between the implanted recoil and α decay of ^{179}Pb within a 20 ms correlation time followed by ^{179}Pb 's child ^{175}Hg α decay within a 45 ms correlation time. The red line is a one-component fit described in Ref. [27] and yields a half-life of $t_{1/2} = 2.7(2)$ ms for ^{179}Pb . The inset shows α -particle energy of ^{179}Pb correlated with ^{175}Hg α decay, which correspond to the time distribution.

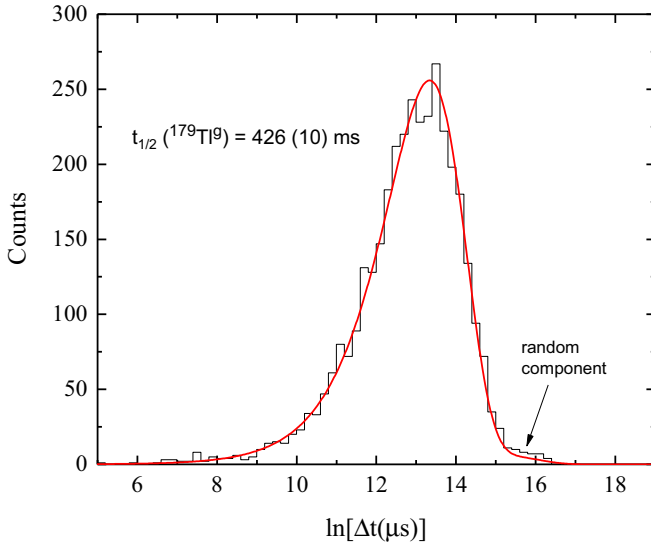


FIG. 4. The logarithmic-time difference (Δt) between the implanted recoil and $^{179}\text{Tl}^g$ α decay. α -particle energy condition of recoil- $\alpha_1(^{179}\text{Tl}^g)$ - $\alpha_2(^{175}\text{Au}^g)$ correlation was required within 12 s and 620 ms searching time of recoil- α_1 and α_1 - α_2 correlations, respectively. The red line is the two-component fit described in Ref. [27] and yields the half-lives of $t_{1/2} = 426(10)$ ms and $t_{1/2} = 2.7(5)$ s for $^{179}\text{Tl}^g$ α decay and the random correlation, respectively.

The α -particle energy of the α -decaying ground state $^{179}\text{Tl}^g$ was deduced from the present work to be $E_\alpha = 6557(4)$ keV. In Fig. 4 the logarithmic-time difference spectrum between the implanted recoils in the DSSDs and the α decay of $^{179}\text{Tl}^g$ is plotted within a 12 s searching time. The gated α -particle energy of $^{179}\text{Tl}^g$ is correlated with the α -decaying child nuclei $^{175}\text{Au}^g$ [14] within a 620 ms searching time. The half-life of $^{179}\text{Tl}^g$ was extracted as $t_{1/2} = 426(10)$ ms using a two-component fit [27]. In the present work, α_1 (parent)- α_2 (child) correlations of $^{179}\text{Tl}^g \rightarrow ^{175}\text{Au}^g$ and $^{179}\text{Tl}^m \rightarrow ^{175}\text{Au}^m$, which were recently reported in Refs. [4,14] were confirmed. Table I shows a comparison of α -particle energies and half-lives of $^{179}\text{Tl}^{g,m}$ and $^{175}\text{Au}^{g,m}$ deduced from the present work and earlier studies.

TABLE I. Comparison between α -particle energies E_α and half-life values $t_{1/2}$ of $^{179}\text{Tl}^{g,m}$ and $^{175}\text{Au}^{g,m}$ isotopes obtained in the present work and the earlier studies.

Isotope	E_α (keV)	$t_{1/2}$ (ms)	Reference
$^{179}\text{Tl}^g$	6557(4)	426(10)	Present work
	6560(4)	265(10)	[14]
	6568 ^a	415(55)	[29]
	6568(18)	430(350)	[22]
$^{179}\text{Tl}^m$	7206(4)	1.40(3)	Present work
	7207(5)	1.46(4)	[4]
$^{175}\text{Au}^g$	6433(4)	200(3)	Present work
	6433(4)	207(7)	[14]
$^{175}\text{Au}^m$	6433(4)	136(1)	Present work
	6432(5)	138(5)	[4]

^aNo uncertainty value was given.

Figure 5(a) shows the summed (clover and planar Ge detectors) γ -ray energy spectrum within a $1 \mu\text{s}$ of a recoil implant, which was prior to the ground state α decay [$E_\alpha = 6557(4)$ keV] of $^{179}\text{Tl}^g$ within a 1.4 s correlation time of a recoil. The spectrum is dominated by the known γ -ray transitions in ^{177}Hg [28] and Hg x rays, while γ -ray peaks marked with an asterisk are the newly observed transitions feeding the ground state of ^{179}Tl . The inset in Fig. 5(a) shows the correlated α -particle spectrum collected within a 1.4 s correlation time after a recoil implant. This figure displays the overlap between the α -decay characteristics of $^{179}\text{Tl}^g$ [$E_\alpha = 6557(4)$ keV, $t_{1/2} = 426(10)$ ms] and ^{177}Hg [28] [$E_\alpha = 6577(9)$ keV, $t_{1/2} = 114(15)$ ms].

In order to exclude the contribution of ^{177}Hg , recoils correlated with $\alpha_1(^{179}\text{Tl}^g)$ and $\alpha_2(^{175}\text{Au}^g)$ decays were required, as is shown in Fig. 5(b). The inset shows the α_1 -decay activity correlated with $\alpha_2(^{175}\text{Au}^g)$. The maximum searching time for recoil- α_1 and α_1 - α_2 is 1.4 s and 620 ms, respectively. In addition, the α decay of $^{179}\text{Tl}^m$ [4] is observed as well, since its child α decay of $^{175}\text{Au}^m$ [14] [$E_\alpha = 6433(4)$ keV, $t_{1/2} = 136(1)$ ms] has overlapping decay properties with that of $^{175}\text{Au}^g$ [$E_\alpha = 6433(4)$ keV, $t_{1/2} = 200(3)$ ms].

In Fig. 5(b) γ -ray peaks of 94.0(5) keV, 226.0(6) keV, and 584.5(5) keV are evident. These transitions are subsequent to the decay of an isomeric state, which finally feeds the ground state of $^{179}\text{Tl}^g$. Thallium K -shell x rays having energies of $K_{\alpha 1} = 72.87$ keV and $K_{\alpha 2} = 70.83$ keV [26] can also be seen in Fig. 5(b) as a composite peak due to the resolution of the Ge detectors.

The low statistics related to γ -ray transitions feeding the ground state of $^{179}\text{Tl}^g$ did not allow a recoil- $[\gamma-\gamma]$ coincidence analysis. The intensity ratio of (I_{K_α}/I_{94}) < 1 for the 94 keV transition firmly assigns this transition to have an $E1$ character, due to the fact that $\alpha_{\text{tot}}(E1) = \lambda_e/\lambda_\gamma = 0.500(7)$ [25] and any other multipolarity for this energy has an α_{tot} more than an order of magnitude greater than this value. The 226 keV and 584.5 keV transitions are then assigned multiplicities of $M1$ and $E2$ with total internal-conversion coefficients [25] of $\alpha_{\text{tot}}(M1) = 0.856(12)$ and $\alpha_{\text{tot}}(E2) = 0.0193(3)$, respectively. The assignments are based on the assumption that all the three transitions form a cascade, where their intensities must balance within errors, as shown in Table II. For no other combination of multiplicities do the intensities balance. Moreover, the total Tl x-ray yield, relative to the γ -ray yield, deduced from Fig. 5(b) supports the aforementioned multipolarity assignments. In the present work, in total three transitions of 94.0(5) keV, 584.5(5) keV, and 226.0(6) keV were observed for the first time to depopulate the newly observed isomeric state in ^{179}Tl .

Half-lives of $t_{1/2} = 112_{-15}^{+20}$ ns, $t_{1/2} = 130_{-30}^{+50}$ ns, and $t_{1/2} = 100_{-30}^{+50}$ ns were measured for the 94 keV, 226 keV, and 584.5 keV transitions, respectively, using the maximum-likelihood method within a $1 \mu\text{s}$ searching time. These values are consistent within errors proving that all transitions are delayed by the depopulation of the same isomeric state. The weighted-average half-life value for the isomeric state is $t_{1/2} = 114_{-10}^{+18}$ ns.

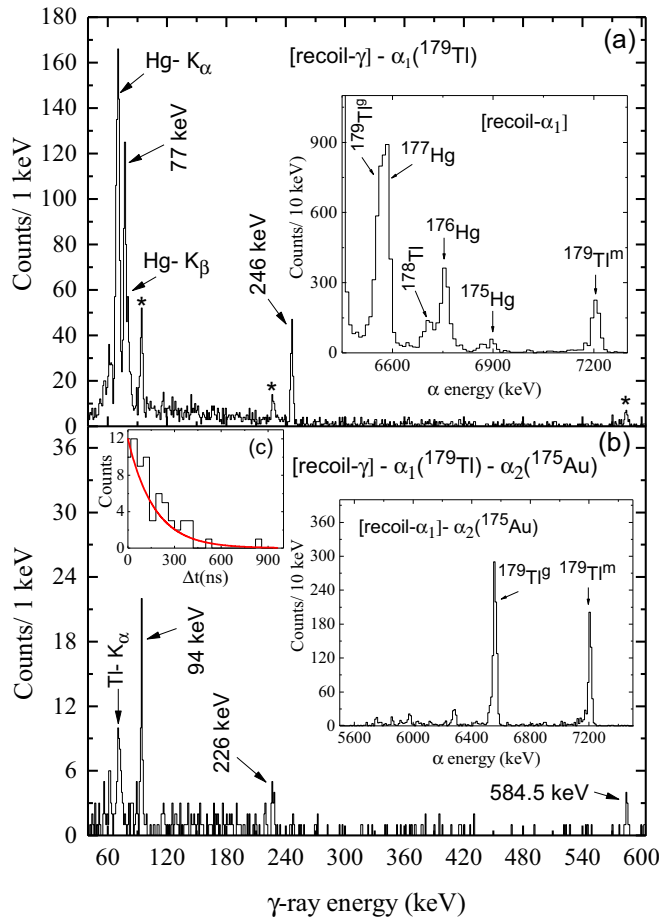


FIG. 5. Summed energy spectra of γ rays detected in the GREAT planar Ge and clover detectors within $1 \mu\text{s}$ of a recoil implantation in the DSSDs. (a) γ -ray spectrum correlated with $\alpha_1(^{179}\text{Tl}^g)$ decays, where the recoil- α_1 correlation time is 1.4 s. The inset reveals correlated α decay within 1.4 s of a recoil implant in the DSSD pixel. (b) γ -ray spectrum correlated with $\alpha_1(^{179}\text{Tl}^g)$ decay followed by $\alpha_2(^{175}\text{Au}^g)$, where recoil- α_1 and α_1 - α_2 correlation times are 1.4 s and 620 ms, respectively. The inset figure shows correlated α decays preceding the $^{175}\text{Au}^g$ α decay within a 620 ms correlation time. (c) Summed decay curve of the 94.0(5) keV, 226.0(6) keV, and 584.5(5) keV transitions. The red line is an exponential distribution plotted using the weighted-average half-life value of $t_{1/2} = 114_{-10}^{+18}$ ns (see the text for details).

There is a known α -decaying isomeric state with a spin and parity of $I^\pi = (11/2^-)$ in $^{179}\text{Tl}^m$ [4]. While the excitation energy of this state is still unknown the α -particle energy and half-life were deduced from this work as $E_\alpha = 7206(4)$ keV and $t_{1/2} = 1.40(3)$ ms, respectively, (see Table I). A search was performed to ascertain the order in excitation energy of the newly observed $t_{1/2} = 114_{-10}^{+18}$ ns isomeric state and the $11/2^-$ state and whether there are transitions between these two states. Searches for [recoil- γ]- $\alpha_1(^{179}\text{Tl}^m)$ and [recoil- e^-]- $\alpha_1(^{179}\text{Tl}^m)$ correlations were performed, where e^- are conversion-electron events correlated with its recoil in the same pixel in the DSSDs. Furthermore, a [recoil- e^-]- $\alpha_1(^{179}\text{Tl}^g)$ correlation was performed. No correlations or coincidences were found. The results show that the 94 keV, 226 keV, and 584.5 keV γ -ray

TABLE II. The energies E_γ of γ -ray transitions observed in both the clover and planar Ge detector of the GREAT spectrometer, which are depopulating the isomeric state in ^{179}Tl . The total transition intensities I_{tot} were calculated taking into account the total internal-conversion coefficients α_{tot} . Both the total transition intensities I_{tot} and γ -ray intensities I_γ are corrected for the clover and planar Ge detector efficiencies and normalized such that $I_\gamma(94 \text{ keV})$ and $I_{\text{tot}}(94 \text{ keV})$ are 100. The measured half-lives $t_{1/2}$ were calculated using the maximum-likelihood method.

E_γ (keV)	I_γ (%)	I_{tot} (%)	$t_{1/2}$ (ns)	Multipolarity
94.0(5)	100(25)	100(25)	112_{-15}^{+20}	$E1$
226.0(6)	65(25)	80(30)	130_{-30}^{+50}	$M1$
584.5(5)	120(50)	80(30)	100_{-30}^{+50}	$(E2)$

transitions only feed the $^{179}\text{Tl}^g$ not the $^{179}\text{Tl}^m$ and that there is no evidence for transitions between the two isomeric states, within the sensitivity limits of the detector set-up used for these measurements.

IV. DISCUSSION

A. Decay spectroscopy of ^{179}Pb

The hindrance factor HF for a $\Delta l = 0$ transition was calculated using the Rasmussen method [30] and corresponds to an unhindered (favored) transition with $\text{HF} = t_{1/2}^{\text{exp}}/t_{1/2}^{\text{ras}} = 1.70(1)$, where $t_{1/2}^{\text{exp}}$ is the experimental half-life from this work and $t_{1/2}^{\text{ras}}$ is the theoretical α -decay half-life. The α -decay reduced width of the $9/2^- \rightarrow 9/2^-$ α decay of ^{179}Pb , $\delta_\alpha^2 = \lambda_{\text{exp}} \times h/p = 44(3)$ keV, for the α -particle energy of $E_\alpha = 7348(5)$ keV was deduced with the assumption of a $\Delta l = 0$, where h is Planck's constant and p is the barrier penetration factor calculated using the WKB approximation. This value is consistent within errors with the value of $\delta_\alpha^2 = 37(4)$ keV for the $\Delta l = 0$ decay of the neighboring odd- A lead nucleus, ^{181}Pb [31]. Table III shows a comparison of different α -decay properties for ^{179}Pb obtained from the present work and from Ref. [4].

A prediction of the ground state configuration of ^{179}Pb was made by Andreyev *et al.* [4] based on the broad distribution of the α -particle energies assigned to ^{179}Pb . The present results confirm this assignment not only with the observation of coincidences between the 7348(5) keV α decay in ^{179}Pb and the 80 keV γ -ray transition from the $9/2^-$ excited state in ^{175}Hg , but also with the α -decay hindrance factor and reduced width supporting a $\Delta l = 0$ decay.

TABLE III. Comparison of α -particle energies E_α , half-life values $t_{1/2}$, and α -reduced widths δ_α^2 for ^{179}Pb nuclei from the present work and from Ref. [4]

E_α (keV)	$t_{1/2}$ (ms)	δ_α^2 (keV)	Reference
7348(5)	2.7(2)	44(3)	present work
7350(20)	$3.5_{-0.8}^{+1.4}$	33_{-10}^{+14}	[4]

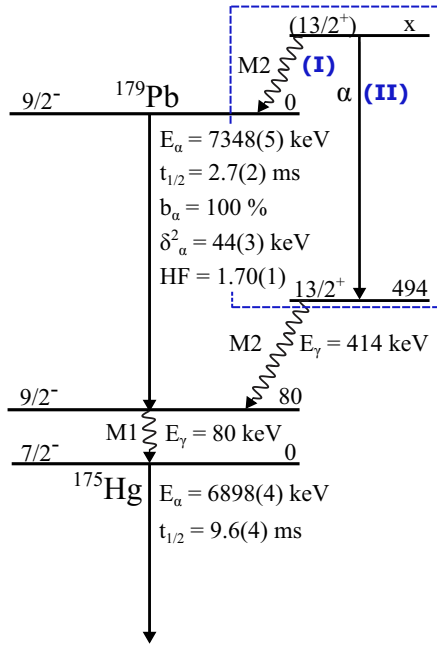


FIG. 6. Decay scheme of ^{179}Pb and ^{175}Hg deduced in the present work, where E_α , E_γ , b_α , δ_α^2 , and HF represent the α -particle energy, γ -ray energy, branching ratio, α -decay reduced width, and the hindrance factor, respectively. The $13/2^+$ excited state in ^{175}Hg at 494 keV is taken from Ref. [5]. The dashed blue box shows the two possible decay-mode scenarios (I) and (II) for the $13/2^+$ state in ^{179}Pb , which are discussed in the text.

Figure 6 shows the decay scheme of ^{179}Pb including the information obtained from this work, and the values for ^{175}Hg taken from the present work and from Ref. [5]. A direct ground state to ground state α decay should be considered, which would have an energy of 7428(5) keV. Disentangling these decays from the α -particle and electron energy sum is practically impossible and the lack of any extra events around this energy leads to the conclusion that such a decay is not observed in the present data set.

In the Pb region the $\nu i_{13/2}$ unique-parity intruder orbital should exist near the Fermi surface. This state has been studied down the α -decay chain of ^{179}Pb in Refs. [3,5] and was also observed in ^{151}Er [32]. It is also observed in the Pb isotopic chain down to ^{183}Pb , where the excitation energy is rather low 79(6) keV [33], but to date has not yet been observed in ^{181}Pb .

If such an isomeric state exists in ^{179}Pb it will have a spin and parity of $I^\pi = 13/2^+$ and will decay in one of two ways as is shown in Fig. 6. The first and most probable scenario (I) is that it feeds the $9/2^-$ ground state of ^{179}Pb via an $M2$ transition. The other possibility (II) is that it α decays to the $13/2^+$ state in ^{175}Hg at an excitation energy of 494 keV, which is depopulated by the cascade of a 414 keV and a 80 keV transition to the ground state of ^{175}Hg as mentioned in Ref. [5]. The electromagnetic transition will dominate over α decay, due to the partial half-life being ~ 1000 times shorter than the α decay for any excitation energy of the $13/2^+$ state. The α -decay partial half-lives for different Q values were calculated using the Geiger-Nuttall law, where $A(Z)$ and $B(Z)$ coefficients are ob-

tained from Ref. [34]. However, as no electromagnetic transition of [$13/2^+$ (isomeric state) $\rightarrow 9/2^-$ (^{179}Pb ground state)] was observed an upper observational transition energy limit of $E \simeq 300$ keV has been set for such a decay based on the flight time through the RITU separator. A lower limit of the transition energy, $E \simeq 180$ keV, was deduced taking into account the statistics and the detection efficiency of γ rays and conversion electrons. The γ -ray transition half-life was calculated using the Weisskopf estimate with the assumption that an $M2$ transition is approximately hindered by a factor of 5–10 in this region, as reported in Ref. [3]. The theoretical total internal-conversion coefficient for an $M2$ transition in ^{179}Pb was obtained from Ref. [25]. Hence the excitation energy of the $13/2^+$ state in ^{179}Pb is not within the range of 180–300 keV.

B. Proton ($9/2^-$) intruder state in ^{179}Tl

Figure 7 provides a partial level scheme of γ -ray transitions feeding the ground state of $^{179}\text{Tl}_{98}$, deduced in the present work. The ground state of odd- A thallium isotopes $^{181-201}\text{Tl}$ are known to have a spin and parity of $I^\pi = 1/2^+$, originating from the $\pi(s_{1/2})^{-1}$ configuration. Recently, the ground state spin of ^{179}Tl has been assigned as $I = 1/2$ using laser spectroscopy by Barzakh *et al.* [11]. In the present work the 226 keV level has been assigned as $I^\pi = (3/2^+)$ as can be seen in Fig. 7 and de-excited by an $M1$ transition to the $1/2^+$ ground state. The $(3/2^+)$ state is associated with a $\pi(d_{3/2})^{-1}$ configuration. This assignment is based on the fact that an excitation energy of 226 keV fits the systematics of $\pi(d_{3/2})^{-1}$ states along the odd- A Tl isotopic chain (see Fig. 8). The 584 keV transition energy is close to the $2^+ \rightarrow 0^+$ transition energy of 558.5 keV in the ^{178}Hg [35] core. Hence the 584.5 keV transition is assigned as a $(7/2^+) \rightarrow (3/2^+)$ transition of $E2$

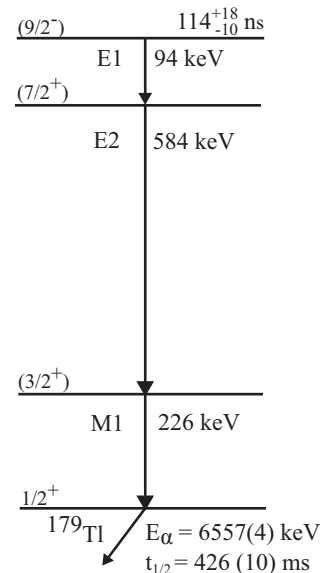


FIG. 7. A partial level scheme of ^{179}Tl proposed in the present work based on assumptions discussed in the text.

character, where the $(7/2^+)$ state can be understood as a $\pi d_{3/2}$ proton-hole coupled to the 2^+ state of the ^{178}Hg core.

The origin of the isomeric state must now be considered. In odd- A thallium isotopes $^{181-201}\text{Tl}$, a $1p-2h$ $\pi h_{9/2}$ intruder state associated with an oblate shape is well known through the observation of low-lying $9/2^-$ isomeric states. Therefore, in ^{179}Tl the 94 keV $E1$ transition is assigned to de-excite a $(9/2^-)$ state and feed the $(7/2^+)$ state, as is shown in Fig. 7. In heavier Tl isotopes $^{195-201}\text{Tl}$ and in ^{181}Tl the $9/2^-$ state decays via an $E3$ transition to a $3/2^+$ excited state, all having comparable $B(E3)$ values as reported in Ref. [10]. However, in lighter odd- A Tl isotopes the excitation energies of the $9/2^-$ state were deduced mainly based on the Bi isotopes α -decay fine structure as reported in Refs. [36–38], with the exception of ^{185}Tl [21]. In the case of ^{179}Tl the $(9/2^-)$ intruder state decays via an $E1$ transition, where the reduced-transition probability of $B(E1) = 1.50^{+23}_{-13} \times 10^{-6}$ W.u. was extracted. This is in good agreement with typical experimental $B(E1)$ values for known delayed $E1$ transitions in this region [6,39–41].

The excitation energy of the $(9/2^-)$ intruder state in the odd- A Tl isotopes has been discussed previously down to ^{181}Tl in Refs. [7,10,38]. In Fig. 8 these systematics are extended as a function of neutron number down to $N = 98$, $A = 179$. The excitation energy of the $(3/2^+)$, $(7/2^+)$, and $(9/2^-)$ states in ^{179}Tl were obtained from the present work. Figure 8 shows that the excitation energy of the $(3/2^+)$ $\pi(d_{3/2})^{-1}$ state follows very well the systematic trend. The excitation energy of the α -decaying $\pi(h_{11/2})^{-1}$ isomeric state in ^{179}Tl is still unknown. However, in Refs. [10,14] it was suggested that the excitation energy of the $9/2^-$ intruder state is ~ 300 – 400 keV above the expected position of the $11/2^-$ state. This prediction was made based on two different extrapolations. One being of the parabolic trend of the $9/2^-$ for Tl isotopes of $A = 181$ – 201 and the other being the excitation energy of the $11/2^-$ state in the lightest odd- A Tl isotopes.

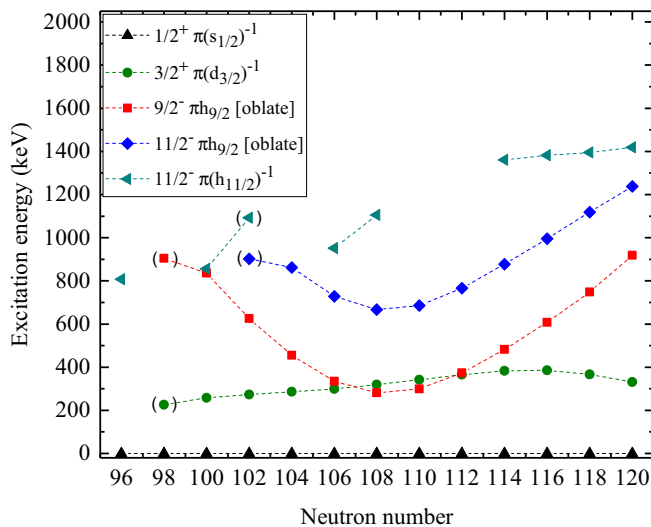


FIG. 8. A plot of the experimental-excitation energies of $9/2^-$, $3/2^+$, and $11/2^-$ states relative to $1/2^+$ ground state in odd- A Tl isotopes as function of neutron numbers. The experimental values are taken from Refs. [10,36,38,43–53], and its from the present work for ^{179}Tl .

In the present work an excitation energy of 904.5(9) keV was deduced for the proton $(9/2^-)$ intruder state. This excitation energy does not follow the parabolic trend of this state along odd-mass $^{179-201}\text{Tl}$ isotopes (see Fig. 8), however it is still increasing as the neutron number decreases beyond the proton drip-line.

At $N = 100$ in the spherical picture both $\nu h_{9/2}$ and the $\nu f_{7/2}$ orbitals are full. Below $N = 100$ the $\nu h_{9/2}$ orbital has empty holes in it. This deviation from the parabolic trend of the $(9/2^-)$ state could be an indication that the proton-neutron interaction by the tensor force [42] between the $\nu h_{9/2}$ state and the spin-orbit partner $\pi h_{11/2}$ and $\pi h_{9/2}$ states will increase the closeness in their individual single-particle energies due to opposing interactions (attraction-repulsion) as the $\nu h_{9/2}$ is emptied.

After finding no evidence of transitions between the newly observed $(9/2^-)$ intruder state and the α -decaying $\pi(h_{11/2})^{-1}$ state, it can be concluded that the excitation energy of these two states is comparable. The fact that there is a transition between the $(9/2^-)$ and $(7/2^+)$ state and the lack of a transition between the $(9/2^-)$ and $11/2^-$ states supports that shape assignments of oblate deformation for the $(7/2^+)$ (2^+ state of ^{178}Hg oblate core [35] + $\pi d_{3/2}$) and the $(9/2^-)$ states and weakly prolate shape for the $11/2^-$ α -decaying state.

Naturally, an $11/2^-$ state member of the band based on oblate-deformed $9/2^-$ intruder state has been observed to follow a similar parabolic trend along odd- A Tl isotopes down to ^{185}Tl and is included in Fig. 8. Below the midshell a deviation from this trend is observed at ^{183}Tl , similar to the deviation presently observed for the $(9/2^-)$ state in ^{179}Tl . Raddon *et al.* [43] speculated that the $\pi(h_{11/2})^{-1}$ state lies lower in the excitation energy than the $11/2^-$ band member below the mid-shell causing this deviation in the parabolic trend. This possibility is indicated by the brackets in Fig. 8.

Clearly, further work with higher statistics and in-beam data for ^{179}Tl is required in order to conduct γ - γ coincidence analysis and to identify different band structures feeding both the isomeric and ground states. This will eliminate the ambiguities in the I^π assignments of the low-lying states.

V. CONCLUSION

In conclusion, this paper reports on the detailed α -decay study of ^{179}Pb having an α -particle energy and half-life of $E_\alpha = 7348(5)$ keV and $t_{1/2} = 2.7(2)$ ms, respectively. The ground-state spin and parity of ^{179}Pb is firmly assigned as $I^\pi = 9/2^-$ based on the prompt coincidence with 80 keV transition in ^{175}Hg and a HF value which corresponds to an unhindered $\Delta l = 0$ transition. In addition, evidence for an isomeric proton $(9/2^-)$ intruder state associated with an oblate shape in ^{179}Tl has been observed for the first time in the present work, having a half-life of $t_{1/2} = 114^{+18}_{-10}$ ns. The excitation energy of 904.5(9) keV has been deduced, which shows a deviation from the parabolic trend of this state around the midshell.

ACKNOWLEDGMENTS

The authors would like to thank John Green from Argonne National Laboratory and B. Lommel and the GSI target laboratory staff for producing the Pd targets. The authors

also thank the GAMMAPOOL European Spectroscopy Resource for the loan of the clovers detector at the GREAT spectrometer. This work has been supported by the Academy of Finland under the Finnish Center of Excellence Program

(contract no. 213503), the Marie Curie Career Integration Grant (No. 304033), the Science and Technology Facilities Council STFC, and by the Academy of Finland (Grant No. 257562).

-
- [1] P. Rakhila, D. G. Jenkins, J. Pakarinen, C. Gray-Jones, P. T. Greenlees, U. Jakobsson, P. Jones, R. Julin, S. Juutinen, S. Ketelhut *et al.*, *Phys. Rev. C* **82**, 011303(R) (2010).
- [2] A. Andreyev, M. Huyse, P. Van Duppen, L. Weissman, D. Ackermann, J. Gerl, F. Hessberger, S. Hofmann, A. Kleinböhl, G. Münzenberg *et al.*, *Nature* **405**, 430 (2000).
- [3] C. Scholey, K. Andgren, L. Bianco, B. Cederwall, I. G. Darby, S. Eeckhauudt, S. Ertürk, M. B. G. Hornillos, T. Grahn, P. T. Greenlees *et al.*, *Phys. Rev. C* **81**, 014306 (2010).
- [4] A. N. Andreyev, S. Antalic, D. Ackermann, T. E. Cocolios, V. F. Comas, J. Elseviers, S. Franchoo, S. Heinz, J. A. Heredia, F. P. Hessberger *et al.*, *J. Phys. G: Nucl. Part. Phys.* **37**, 035102 (2010).
- [5] D. O'Donnell, J. Simpson, C. Scholey, T. Bäck, P. T. Greenlees, U. Jakobsson, P. Jones, D. T. Joss, D. S. Judson, R. Julin *et al.*, *Phys. Rev. C* **79**, 051304(R) (2009).
- [6] G. Lane, G. Dracoulis, A. Byrne, P. Walker, A. Baxter, J. Sheikh, and W. Nazarewicz, *Nucl. Phys. A* **586**, 316 (1995).
- [7] M. Muikku, P. T. Greenlees, K. Hauschild, K. Helariutta, D. G. Jenkins, P. Jones, R. Julin, S. Juutinen, H. Kankaanpää, N. S. Kelsall *et al.*, *Phys. Rev. C* **64**, 044308 (2001).
- [8] W. Reviol, M. Carpenter, U. Garg, R. Janssens, I. Ahmad, I. Bearden, P. Benet, P. Daly, M. Drigert, P. Fernandez *et al.*, *Nucl. Phys. A* **548**, 331 (1992).
- [9] M.-G. Porquet, A. J. Kreiner, F. Hannachi, V. Vanin, G. Bastin, C. Bourgeois, J. Davidson, M. Debray, G. Falcone, A. Korichi *et al.*, *Phys. Rev. C* **44**, 2445 (1991).
- [10] A. N. Andreyev, S. Antalic, D. Ackermann, T. E. Cocolios, V. F. Comas, J. Elseviers, S. Franchoo, S. Heinz, J. A. Heredia, F. P. Heßberger *et al.*, *Phys. Rev. C* **80**, 024302 (2009).
- [11] A. E. Barzakh, A. N. Andreyev, T. E. Cocolios, R. P. de Groot, D. V. Fedorov, V. N. Fedosseev, R. Ferrer, D. A. Fink, L. Ghys, M. Huyse *et al.*, *Phys. Rev. C* **95**, 014324 (2017).
- [12] M. Leino, J. Äystö, T. Enqvist, P. Heikkinen, A. Jokinen, M. Nurmia, A. Ostrowski, W. H. Trzaska, J. Uusitalo, K. Eskola *et al.*, *Nucl. Instrum. Methods Phys. Res. B* **99**, 653 (1995).
- [13] R. D. Page, A. N. Andreyev, D. E. Appelbe, P. A. Butler, S. J. Freeman, P. T. Greenlees, R. D. Herzberg, D. G. Jenkins, G. D. Jones, P. Jones *et al.*, *Nucl. Instrum. Methods Phys. Res. B* **204**, 634 (2003).
- [14] A. N. Andreyev, V. Liberati, S. Antalic, D. Ackermann, A. Barzakh, N. Bree, T. E. Cocolios, J. Diriken, J. Elseviers, D. Fedorov *et al.*, *Phys. Rev. C* **87**, 054311 (2013).
- [15] C. M. Baglin, *Nucl. Data Sheets* **110**, 265 (2009).
- [16] B. Singh, *Nucl. Data Sheets* **75**, 199 (1995).
- [17] G. Duchêne, F. Beck, P. Twin, G. de France, D. Curien, L. Han, C. Beausang, M. Bentley, P. Nolan, and J. Simpson, *Nucl. Instrum. Methods Phys. Res. A* **432**, 90 (1999).
- [18] I. H. Lazarus, D. E. Appelbe, P. A. Butler, P. J. Coleman-Smith, J. R. Cresswell, S. J. Freeman, R. D. Herzberg, I. Hibbert, D. T. Joss, S. C. Letts *et al.*, *IEEE Trans. Nucl. Sci.* **48**, 567 (2001).
- [19] P. Rakhila, *Nucl. Instrum. Methods Phys. Res. A* **595**, 637 (2008).
- [20] H. Badran, C. Scholey, K. Auranen, T. Grahn, P. T. Greenlees, A. Herzan, U. Jakobsson, R. Julin, S. Juutinen, J. Konki *et al.*, *Phys. Rev. C* **94**, 054301 (2016).
- [21] Evaluated Nuclear Structure Data File (ENSDF), access via <http://www.nndc.bnl.gov/ensdf/>.
- [22] R. D. Page, P. J. Woods, R. A. Cunningham, T. Davinson, N. J. Davis, A. N. James, K. Livingston, P. J. Sellin, and A. C. Shotton, *Phys. Rev. C* **53**, 660 (1996).
- [23] J. Uusitalo, M. Leino, R. Allatt, T. Enqvist, K. Eskola, P. Greenless, S. Hurskanen, A. Keenan, H. Kettunen, P. Kuusiniemi *et al.*, *Z. Phys. A* **358**, 375 (1997).
- [24] J. Sarén, J. Uusitalo, M. Leino, and J. Sorri, *Nucl. Instrum. Methods Phys. Res. A* **654**, 508 (2011).
- [25] T. Kibedi, T. Burrows, M. Trzhaskovskaya, P. M. Davidson, and C. W. Nestor, *Nucl. Instrum. Methods Phys. Res. A* **589**, 202 (2008).
- [26] R. B. Firestone, V. S. Shirley, C. M. Baglin *et al.*, *The 8th Edition of the Table of Isotopes* (Springer, Hungary, 1997), Vol. 29.
- [27] K. H. Schmidt, *Eur. Phys. J. A* **8**, 141 (2000).
- [28] A. Melarangi, D. Appelbe, R. D. Page, H. J. Boardman, P. T. Greenlees, P. Jones, D. T. Joss, R. Julin, S. Juutinen, H. Kettunen *et al.*, *Phys. Rev. C* **68**, 041301(R) (2003).
- [29] M. W. Rowe, J. C. Batchelder, T. N. Ginter, K. E. Gregorich, F. Q. Guo, F. P. Hessberger, V. Ninov, J. Powell, K. S. Toth, X. J. Xu *et al.*, *Phys. Rev. C* **65**, 054310 (2002).
- [30] J. O. Rasmussen, *Phys. Rev.* **113**, 1593 (1959).
- [31] A. N. Andreyev, S. Antalic, D. Ackermann, T. E. Cocolios, V. F. Comas, J. Elseviers, S. Franchoo, S. Heinz, J. A. Heredia, F. P. Heßberger *et al.*, *Phys. Rev. C* **80**, 054322 (2009).
- [32] T. Fukuchi, T. Hori, T. Masue, K. Tajiri, A. Sato, T. Furukawa, A. Odahara, T. Shimoda, Y. Wakabayashi, Y. Gono *et al.*, *Eur. Phys. J. A* **39**, 49 (2009).
- [33] D. G. Jenkins, A. N. Andreyev, R. D. Page, M. P. Carpenter, R. V. F. Janssens, C. J. Lister, F. G. Kondev, T. Enqvist, P. T. Greenlees, P. M. Jones *et al.*, *Phys. Rev. C* **66**, 011301(R) (2002).
- [34] C. Qi, A. Andreyev, M. Huyse, R. Liotta, P. V. Duppen, and R. Wyss, *Phys. Lett. B* **734**, 203 (2014).
- [35] F. G. Kondev, R. V. F. Janssens, M. P. Carpenter, K. Abu Saleem, I. Ahmad, M. Alcorta, H. Amro, P. Bhattacharyya, L. T. Brown, J. Caggiano *et al.*, *Phys. Rev. C* **62**, 044305 (2000).
- [36] A. N. Andreyev, S. Antalic, D. Ackermann, S. Franchoo, F. P. Heßberger, S. Hofmann, M. Huyse, I. Kojouharov, B. Kindler, P. Kuusiniemi *et al.*, *Phys. Rev. C* **73**, 044324 (2006).
- [37] J. Batchelder, K. Toth, C. Bingham, L. Brown, L. Conticchio, C. Davids, R. Irvine, D. Seweryniak, W. Walters, J. Wauters *et al.*, *Eur. Phys. J. A* **5**, 49 (1999).
- [38] E. Coenen, K. Deneffe, M. Huyse, P. Van Duppen, and J. L. Wood, *Phys. Rev. Lett.* **54**, 1783 (1985).
- [39] S. V. Rigby, D. M. Cullen, P. J. R. Mason, D. T. Scholes, C. Scholey, P. Rakhila, S. Eeckhauudt, T. Grahn, P. Greenlees, P. M. Jones *et al.*, *Phys. Rev. C* **78**, 034304 (2008).
- [40] T. Lönnroth, *Z. Phys. A - Atomic Nuclei* **331**, 11 (1988).

- [41] M. Venhart, A. Andreyev, J. Wood, S. Antalic, L. Bianco, P. Greenlees, U. Jakobsson, P. Jones, R. Julin, S. Juutinen *et al.*, *Phys. Lett. B* **695**, 82 (2011).
- [42] T. Otsuka, T. Suzuki, R. Fujimoto, H. Grawe, and Y. Akaishi, *Phys. Rev. Lett.* **95**, 232502 (2005).
- [43] P. M. Raddon, D. G. Jenkins, C. D. O'Leary, A. J. Simons, R. Wadsworth, A. N. Andreyev, R. D. Page, M. P. Carpenter, F. G. Kondev, T. Enqvist *et al.*, *Phys. Rev. C* **70**, 064308 (2004).
- [44] F. Kondev, *Nucl. Data Sheets* **108**, 365 (2007).
- [45] B. Singh, *Nucl. Data Sheets* **108**, 79 (2007).
- [46] X. Huang and C. Zhou, *Nucl. Data Sheets* **104**, 283 (2005).
- [47] H. Xiaolong and K. Mengxiao, *Nucl. Data Sheets* **121**, 395 (2014).
- [48] M. Shamsuzzoha Basunia, *Nucl. Data Sheets* **143**, 1 (2017).
- [49] V. Vanin, N. Maidana, R. Castro, E. Achterberg, O. Capurro, and G. Marti, *Nucl. Data Sheets* **108**, 2393 (2007).
- [50] T. Johnson and B. Singh, *Nucl. Data Sheets* **142**, 1 (2017).
- [51] M. Basunia, *Nucl. Data Sheets* **110**, 999 (2009).
- [52] M. P. Carpenter, F. G. Kondev, and R. V. F. Janssens, *J. Phys. G: Nucl. Part. Phys.* **31**, S1599 (2005).
- [53] G. Poli, C. Davids, P. Woods, D. Seweryniak, J. Batchelder, L. Brown, C. Bingham, M. Carpenter, L. Conticchio, T. Davinson *et al.*, *Phys. Rev. C* **59**, R2979 (1999).